H_2O_2-Treated Actin: Assembly and Polymer Interactions with Cross-Linking Proteins

Isabella DalleDonne, Aldo Milzani, and Roberto Colombo
Department of Biology, University of Milan, 20133 Milan, Italy

ABSTRACT During inflammation, hydrogen peroxide, produced by polymorphonuclear leukocytes, provokes cell death mainly by disarranging filamentous (polymerized) actin (F-actin). To show the molecular mechanism(s) by which hydrogen peroxide could alter actin dynamics, we analyzed the ability of H_2O_2-treated actin samples to polymerize as well as the suitability of actin polymers (from oxidized monomers) to interact with cross-linking proteins. H_2O_2-treated monomeric (globular) actin (G-actin) shows an altered time course of polymerization. The increase in the lag phase and the lowering in both the polymerization rate and the polymerization extent have been evidenced. Furthermore, steady-state actin polymers, from oxidized monomers, are more fragmented than control polymers. This seems to be ascribable to the enhanced fragility of oxidized filaments rather than to the increase in the nucleation activity, which markedly falls. These facts, along with the unsuitability of actin polymers from oxidized monomers to interact with both filamin and α-actinin, suggest that hydrogen peroxide influences actin dynamics mainly by changing the F-actin structure. H_2O_2, via the oxidation of actin thiols (in particular, the sulfhydryl group of Cys-374), likely alters the actin C-terminus, influencing both subunit/subunit interactions and the spatial structure of the binding sites for cross-linking proteins in F-actin. We suggest that most of the effects of hydrogen peroxide on actin could be explained in the light of the "structural connectivity," demonstrated previously in actin.

INTRODUCTION

During phlogosis, oxidants and proteases are massively produced by stimulated polymorphonuclear leukocytes. Parenchimal cells (such as epithelial cells, skeletal muscle cells, neurons, etc.) do not participate in the phlogistic event but, because of the influence exerted by local environmental changes, they show focal regressive phenomena that could lead to cell death.

Hydrogen peroxide is the major oxidant generated from superoxide produced by activated polymorphonuclear leukocytes. H_2O_2 causes cell lysis within a few hours after exposure (Nathan et al., 1979; Simon et al., 1981; Weiss et al., 1981; Sacks et al., 1978; Martin, 1984). Several events occur with oxidant injury to cells (Schraufstatter et al., 1985, 1986; Spragg et al., 1985; Bellomo et al., 1982; Trump and Mergner, 1974; Jewell et al., 1982). Among these, the onset of characteristic changes in the cell surface morphology (so-called plasma membrane blebbing) suggests that cytoskeletal elements of the cell cortex (mostly microfilaments) could represent one of the cellular targets of the hydrogen peroxide biological activity (Mirabelli et al., 1988). The relationship between blebbing and damage to actin filaments is supported by the findings that two actin poisons, cytochalasin B and phalloidin, are able to cause bleb formation in hepatocytes (Mesland et al., 1981; Prentki et al., 1979). Marked changes in filamentous (polymerized) actin (F-actin) organization follow cell treatments with oxidants. After cell exposure to hydrogen peroxide, microfilaments appear to be shortened and collapsed into small bundles (Hinshaw et al., 1986, 1991). Moreover, the cell F-actin content seems to increase, but it is not clear what conditions are able to promote this kind of cellular response. From Hinshaw et al. (1991), the increase in cytoplasmic F-actin is primarily related to the condition under which sulfhydryl oxidation occurs. Furthermore, Omann et al. (1994) suggested that the increase in polymeric actin, after oxidative cell injury, is not related to an increase in actin nucleation activity (which, on the contrary, significantly falls), but it is probably ascribable to an enhanced release of actin monomers from monomeric (globular) actin (G-actin)-sequestering proteins, such as profilin and thymosin β_4.

Actin assembly in solution, starting from the purified protein, represents a simple system that is easy to control and which shares most of the properties shown by polymeric actin formation in the cytoplasm. We used the polymerization of pure actin in solution as a suitable tool for the clarification of the molecular mechanism(s) driving the hydrogen peroxide activity on G-actin/F-actin equilibrium. Finally, we tested the ability of actin polymers, produced by the assembly of oxidized monomers, to build three-dimensional actin structures.

Received for publication 17 April 1995 and in final form 30 August 1995.

Address reprint requests to Dr. Roberto Colombo, Department of Biology, University of Milan, Chair of Cytology and Histology, Via Celoria 26, 20133 Milan, Italy. Tel.: +39 2 266 04 474; Fax: +39 2 266 04 462; E-mail: parsifal@imiucca.csi.unimi.it.

0006-3495/95/12/2710/10 $2.00

MATERIALS AND METHODS

Reagents

Analytical-grade reagents were used in our experiments. *N*-(1-Pyrenyl)-iodoacetamide was purchased from Molecular Probes (Eugene, OR). ATP, dithiothreitol, hydrogen peroxide, and *N,N'*-1,4-phenylenebismaleimide were purchased from Sigma Chemical Co. (St. Louis, MO).

Preparation of proteins

Actin was prepared from rabbit skeletal muscles according to the method of Spudich and Watt (1971), with an additional Sephadex G-150 gel filtration step. The protein was greater than 99% pure, as checked by sodium dodecylsulfate–polyacrylamide gel electrophoresis (SDS-PAGE). G-actin was stored on ice in 2 mM Tris-HCl (pH 7.5), 0.2 mM ATP, 0.5 mM dithiothreitol, 0.2 mM $CaCl_2$, 1.5 mM NaN_3 (G-buffer) and used within 5 days or lyophilized after the addition of 2 mg sucrose/mg actin (Frieden and Goddette, 1983). G-actin (42.3 kDa) concentration was determined by measuring absorbance at 290 nm, using an extinction coefficient of 0.617 $mg^{-1} \cdot ml \cdot cm^{-1}$ (Gordon et al., 1976).

Smooth muscle α-actinin and filamin were purified from chicken gizzards as described by Feramisco and Burridge (1980) and stored at −20°C in 20 mM Tris-HCl (pH 7.6), 20 mM NaCl, 0.1 mM EDTA, 15 mM β-mercaptoethanol, after the addition of 20% (v/v) glycerol.

Before use, both the protein preparations were dialyzed for 48 h against G-buffer; moreover, α-actinin was centrifuged for 60 min at 100,000 × *g*. α-Actinin (subunit 100 kDa; Suzuki et al., 1976) and filamin (dimer 500 kDa; Wang et al., 1975) concentrations were determined by light absorption, using $E_{278} = 0.97\ mg^{-1} \cdot ml \cdot cm^{-1}$ (Suzuki et al., 1976) and $E_{280} = 1.351\ mg^{-1} \cdot ml \cdot cm^{-1}$ (Shizuta et al., 1976), respectively.

H_2O_2 treatment on actin monomers

G-actin (24–35.5 μM) was treated with various concentrations (5, 10, 20 mM) of H_2O_2 for 30 min, at 25°C. Given that the presence of catalase in our protein solutions was undesirable, the removal of the H_2O_2 was accomplished by gel filtration on Sephadex G-25 according to the method of Holeysovsky and Lazdunski (1968). Measurements of the absorbance at 230 nm showed the complete removal of H_2O_2 from eluates. All reported experiments have been carried on in H_2O_2-free media.

Emission spectra of H_2O_2-treated actin (not shown), after excitation at 300 nm, did not show the spectral redshift that characterizes denatured actin (Kerwar and Lehrer, 1972; Gershman et al., 1988; Kinosian et al., 1993).

Determination of thiols

After oxidation with H_2O_2 and gel filtration on Sephadex G-25, G-actin solutions were lyophilized under vacuum. The lyophilized samples (0.2 mg) were dissolved in 100 μl of 2 mM Tris-HCl (pH 7.5), 0.2 mM ATP, 0.2 mM $CaCl_2$, 1.5 mM NaN_3, containing 1% (w/v) SDS to denature the protein and expose all of its cysteine residues. The presence of SDS does not affect the determination of the number of thiols (Knight and Offer, 1978). Free thiols were determined at 412 nm by reaction with a ~20-fold excess of 5,5′-dithiobis-(2-nitrobenzoic acid) (1 mM in 0.05 M phosphate buffer, pH 7.5), using the extinction coefficient of the thionitrobenzoate ($E_{412} = 13.6\ mM^{-1} \cdot cm^{-1}$; Ellman, 1959).

Fluorescent labeling of actin

N-(1-Pyrenyl)iodoacetamide (pyrene)-actin was prepared as described by Tellam and Frieden (1982). The pyrene-actin concentration and the extent of labeling were determined by measuring absorbance at 290 and 344 nm, using $E_{344} = 2.2 \times 10^4\ M^{-1} \cdot cm^{-1}$ for the protein-dye complex, in agreement with Kouyama and Mihashi (1981) and Cooper et al. (1983). A pyrene/actin molar ratio of 0.8–0.9 was usually obtained.

Actin assembly conditions

G-actin concentration was 12 μM, unless stated otherwise. Polymerization was always induced at 25°C by the addition of KCl and $MgCl_2$, up to a final concentration of 100 mM and 2 mM, respectively.

Pre-formed actin filaments were prepared by polymerizing small aliquots of G-actin (12 μM) in test cuvettes overnight.

Nucleated actin polymerization and depolymerization tests were carried out at salt concentrations that were, respectively, one-quarter and one-tenth of the initial ones (for details, see figure legends).

Before all of the experiments, G-actin solutions were centrifuged for 60 min at 100,000 × *g* to remove small aggregates. Before sample preparation, protein solutions and buffers were filtered with 0.20 μm disposable filters and degassed.

Actin polymerization measurements

Fluorescence measurements

Actin polymerization was monitored at 25°C by measuring the fluorescence enhancement of trace quantities of pyrene-actin (10% of total actin) in a Kontron SFM 25 spectrofluorimeter. In depolymerization experiments, pyrene-actin was 20% of total actin. The excitation and emission wavelengths were 365 and 407 nm, respectively. The spectrofluorimeter was equipped with a neutral density filter (50%) to avoid pyrene-actin photobleaching and a cut-off filter (390 nm) to minimize light scattering. Fluorescence intensity was converted to F-actin concentration based on the calibration curve for fluorescence versus F-actin concentration.

Light-scattering measurements

Actin polymerization was followed at 25°C by the increase in the 90° light-scattering at 546 nm (Wegner and Savko, 1982). Light-scattering intensities were expressed in arbitrary units (a.u.), considering 100 the signal from a standard sample (12 μM G-actin induced to polymerize by the addition of 100 mM KCl + 2 mM $MgCl_2$ for 24 h, at 25°C).

Intermolecular cross-linking during actin polymerization

Actin was covalently cross-linked with *N,N′*-1,4-phenylenebismaleimide (Colombo et al., 1991a,b) according to the method of Millonig et al. (1988). SDS-PAGE (7.5% gels) of cross-linked actin was performed according to the method of Laemmli (1970). Gels were stained with Coomassie brilliant blue R-250.

Light-scattering assay for actin filament bundles

The formation of actin filament bundles was measured at 400 nm under a 90° observation angle, at 25°C (Wilkins and Lin, 1986). The light-scattering intensity was expressed in arbitrary units (a.u.), considering 100 the light-scattering intensity of control samples (9.5 μM G-actin, routinely polymerized, in the presence of 1.0 μM α-actinin).

Low shear viscometry

Apparent viscosity measurements were carried out with a homemade falling-ball apparatus, as described by Pollard and Cooper (1982). Glass capillary tubes (100-μl micropipettes) with an internal diameter of 1.3 mm and stainless-steel balls (material 440 C) with a diameter of 0.64 mm and a density of 7.2 $g\ cm^{-3}$ were used. For measurements, the micropipettes were held at 80° to the orizontal, in a thermostatted water bath, at 25°C. Samples were drawn up into the micropipettes immediately after salt addition, so they were subjected to shear only at the beginning of polymerization. The apparent viscosity of the samples is given in arbitrary units, considering 100 as the apparent viscosity of control samples (7.1 μM G-actin, routinely polymerized, in the presence of 0.095 μM filamin).

Electron microscopy

Protein samples were dispensed in 5-μl aliquots on collodion film-coated grids by truncated pipette tips to avoid filament fragmentation. After 60 s, grids were dried from the side with filter paper and negatively stained with the addition of 5 μl of 1% uranyl acetate. After 10 s, excess stain was removed with filter paper. The staining procedure was repeated five times. Specimens were air dried and observed at 80 kV with a JEOL 100-SX electron microscope.

RESULTS

Free thiols in H_2O_2-treated actin monomers

Native G-actin shows five free thiols, likely ascribable to the five cysteine residues characterizing its primary structure. Under the same conditions, the absorbance at 412 nm of H_2O_2-treated actin samples (Ellman, 1959; for details see Materials and Methods) lowers to three-fifths of that of native actin (Fig. 1), suggesting the lack of two free thiols as a consequence of the oxidative injury. Because hydrogen peroxide is a relatively nonspecific oxidizing agent (Neumann, 1972), not only sulfhydryl groups could be the targets of H_2O_2 on actin molecule. In particular, His-371, at the C-terminus of actin molecule, could represent a further molecular site affected by the hydrogen peroxide activity.

Time course of polymerization from H_2O_2-treated actin monomers

Oxidized actin polimerizes slower than control actin, showing a longer lag phase, a lower maximum rate of assembly, and a reduced polymerization extent. In the H_2O_2-treated samples (5, 10, and 20 mM), the light-scattering intensity, 120 min after the start of polymerization, decreased to 92%, 86%, and 73% of that of controls, respectively. The longer lag phases observed in oxidized actin samples could be explained by the greater time required for actin filaments to reach the minimum size producing a measurable light-scattering signal (Fig. 2 *A*).

The time course of fluorescence changes still shows that oxidized actin polymerizes less efficiently than control actin (Fig. 2 *B*). The lag phase increases (0.6 min for control actin; 0.9, 1.1, and 1.5 min for actin treated with 5, 10, and 20 mM H_2O_2, respectively), and both the maximum rate (1.58 $\mu M \cdot min^{-1}$ for control actin; 1.17, 0.79, and 0.34 $\mu M \cdot min^{-1}$, for 5, 10 and 20 mM H_2O_2-treated actin samples, respectively) and the extent of polymerization (11.7 μM for control actin; 10.8, 10.0, and 9.5 μM, for 5, 10, and 20 mM H_2O_2-treated actin, respectively) decrease with the increase of the oxidative stress.

Effects of monomer oxidation on actin polymerization steps

Nucleation, which highly depends on actin concentration, is the rate-limiting step in spontaneous polymerization of actin monomers (Korn, 1985), being thermodynamically unfavorable (Oosawa and Kasai, 1971); formation of nuclei ac-

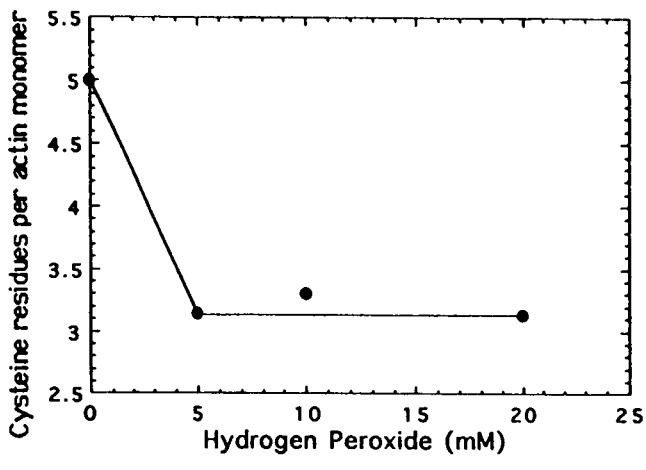

FIGURE 1 Effect of H_2O_2 treatment on actin thiols. The determination of the number of cysteine residues per actin monomer was performed in the presence of 1% (w/v) SDS, according to the method of Knight and Offer (1978), as described in Materials and Methods.

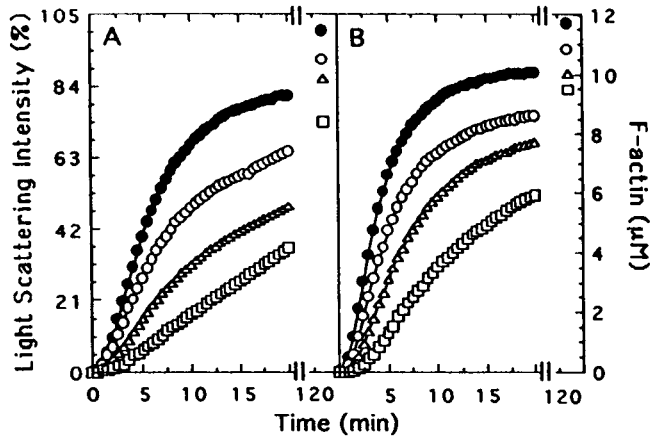

FIGURE 2 Effects of monomer oxidation on the time course of actin polymerization. 24–35.5 μM G-actin (10% pyrene-actin for the fluorometry experiments) was incubated with 0 mM (●, control), 5 mM (○), 10 mM (△), and 20 mM (□) H_2O_2 for 30 min at 25°C and then chromatographed on a small Sephadex G-25 column. (*A*) Polymerization was initiated by the addition of polymerizing salts (see Materials and Methods) to 12 μM G-actin solutions (control and oxidized samples). The light-scattering intensity enhancement was followed over the initial (20 min) time course and at 120 min after initiation of polymerization. The steady-state light scattering intensity (after 120 min from salt addition) for the 5, 10, and 20 mM H_2O_2-treated samples was 92%, 86%, and 73%, respectively, of the control. (*B*) Polymerization was initiated by the addition of polymerizing salts (see Materials and Methods) to 12 μM G-actin solutions (10% pyrene-actin; control and oxidized samples). Changes in fluorescence intensity were followed over the initial (20 min) time course and at 120 min after initiation of polymerization. The lag phase was 0.6 min for control actin, 0.9, 1.1, and 1.5 min for actin treated with 5, 10, and 20 mM H_2O_2, respectively. The maximum polymerization rate was 1.58 $\mu M\ min^{-1}$ for control actin, and 1.17, 0.79, and 0.34 $\mu M\ min^{-1}$ for actin treated with 5, 10, and 20 mM H_2O_2, respectively. The extent of polymerization at 120 min after salt addition was 11.7 μM for control actin, and 10.8, 10.0, and 9.5 μM for actin treated samples, from the lower to the stronger oxidative treatment.

counts for the delay time in polymer formation characterizing early actin assembly. Unfortunately, nucleation can only be studied indirectly. We monitored nucleation of oxidized actin monomers by intermolecular cross-linking with *N,N'*-1,4-phenylenebismaleimide, a bifunctional sulfhydryl reagent (Knight and Offer, 1978), which is able to covalently cross-link Cys-374 on one actin subunit to Lys-191 on the neighboring subunit within incoming actin polymers. Thanks to their different molecular weights, cross-linked actin complexes will then become separable by SDS-PAGE (Millonig et al., 1988; Colombo et al., 1991a,b). Fig. 3 shows that both upper dimers (UDs; apparent molecular mass, of 115 kDa) and higher molecular weight oligomers (HOs; apparent molecular mass, >200 kDa) are fewer and form slower in oxidized actin samples than in controls. The upper dimer, the smallest elongating actin aggregate, is a "suboptimal" nucleus because cross-linked UDs, when added to polymerizing actin samples, shorten, but do not completely abolish, the lag phase (Millonig at al., 1988). UDs represent the long-pitch helix actin dimers, which only define the intersubunit contacts along the two long-pitch helices of the actin filament, but not between them (Millonig et al., 1988). The delay in UD formation could account for assembly difficulties shown by H_2O_2-treated actin monomers.

To analyze the effects of monomer oxidation on elongation, we investigated the growth of pre-formed actin "seeds" after dilution with oxidized G-actin. Fig. 4 shows the elongation of pre-formed actin filaments after the addition of oxidized monomers; the net elongation rates were calculated from the initial rates of fluorescence intensity increases. Elongation of actin "seeds" occurring in the presence of oxidized monomers is slower if compared to that of control samples. Moreover, the slackening of elongation is more evident the higher the oxidant concentration used during monomer treatment. The elongation rate reached 1.55 $\mu M \cdot min^{-1}$ in controls and 0.97, 0.58, and 0.23 $\mu M \cdot min^{-1}$ in actin samples treated with 5, 10, and 20 mM H_2O_2, respectively.

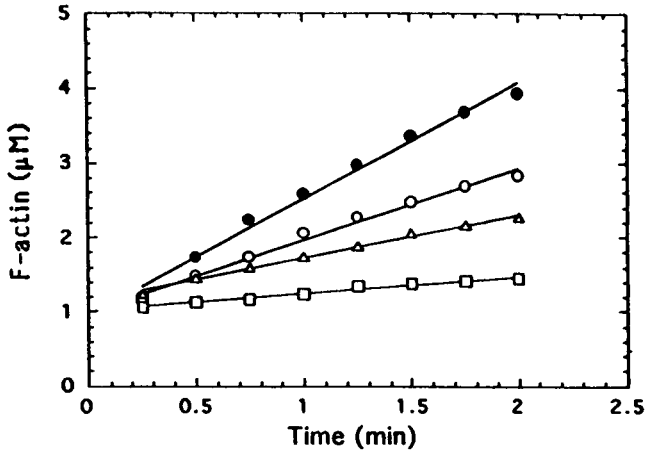

FIGURE 4 Effects of monomer oxidation on the elongation of pre-formed actin filaments. 24–35.5 μM G-actin solutions (10% pyrene-actin) were incubated with 0 mM (●, control), 5 mM (○), 10 mM (△), and 20 mM (□) H_2O_2 as described for Fig. 2. Elongation was started by the addition of 1.5 ml of oxidized G-actin solutions (12 μM) to 0.5 ml aliquots of actin "seeds," prepared as described in Materials and Methods. The final concentrations of polymerizing salts in the elongation assay were 25 mM KCl and 0.5 mM $MgCl_2$. For each sample, the net polymerization rate was calculated from the initial (2 min) rates of fluorescence intensity increases and found to be 1.55 $\mu M\ min^{-1}$ for control actin, and 0.97, 0.58, and 0.23 $\mu M\ min^{-1}$ for actin treated with 5, 10, and 20 mM H_2O_2, respectively.

Finally, the effect of monomer oxidation on the annealing of short actin filaments was examined. It is well established that when actin filaments are mechanically stressed (by

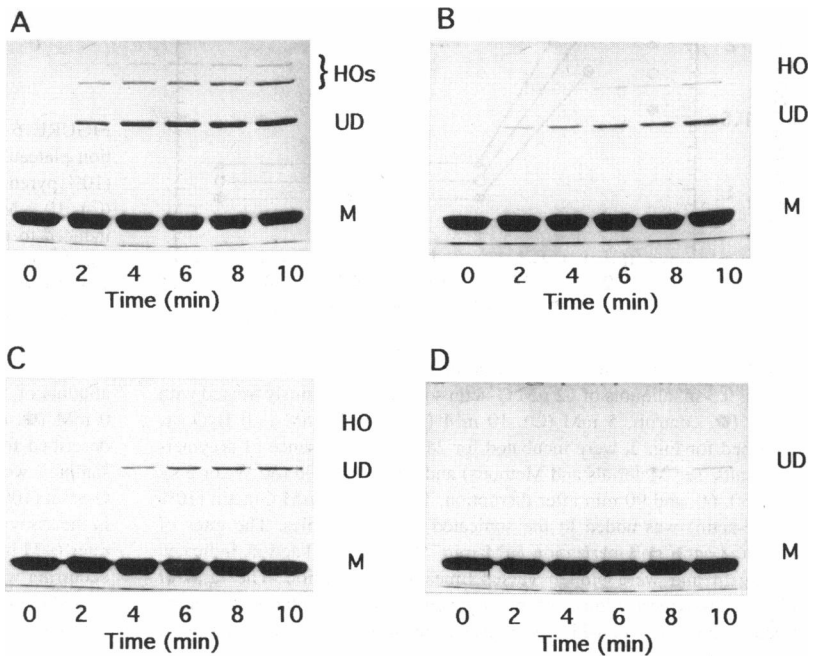

FIGURE 3 Effects of monomer oxidation on actin nucleation. 24 μM G-actin solutions, treated with 0, 5, 10, and 20 mM H_2O_2 as described for Fig. 2, were induced to polymerize by the addition of neutral salts (see Materials and Methods). At the times indicated below each electrophoretic line, polymerizing actin samples were cross-linked with *N,N'*-1,4-phenylenebismaleimide as described in Materials and Methods; cross-linked actin samples were then analyzed by SDS-PAGE. (*A*) control actin; (*B*) actin incubated with 5 mM H_2O_2; (*C*) actin incubated with 10 mM H_2O_2; (*D*) actin incubated with 20 mM H_2O_2. M, monomer; UD, upper dimer; HOs, higher molecular weight oligomers.

sonication, for instance; Nakaoka and Kasai, 1969), they fragment into short pieces, increasing in number. After sonication, steady-state actin samples show a similar distribution of polymer sizes, independent of polymer mass and determined by the energy input (Carlier et al., 1984). After mechanical fragmentation, actin filaments rapidly increase in length and decrease in number, as judged by electron microscopy, viscosity, flow birefringence, and nucleation assays. This suggested the head-to-tail binding of short filaments to form longer polymers (Nakaoka and Kasai, 1969; Kawamura and Maruyama, 1970). Because of the lack of methods for filament length determination in solution, direct evidence for annealing is difficult to obtain (Murphy et al., 1988). We tested indirectly the ability of oxidized actin filaments to anneal by checking the recovery of filament free growing end concentration, at different times after sonication (Fig. 5). Small oxidized G-actin samples were polymerized by the addition of neutral salts, incubated for 24 h, and then sonicated (50 W for 5 s). At the indicated times after sonication, unmodified G-actin (10% pyrene-actin) was added to sonicated oxidized F-actin samples and the rates of fluorescence changes were measured. As shown in Fig. 5, both control and oxidized filaments annealed; all of the samples completely recovered 30 min after sonication. These observations suggest that the annealing step is not significantly affected by oxidation of actin filament subunits.

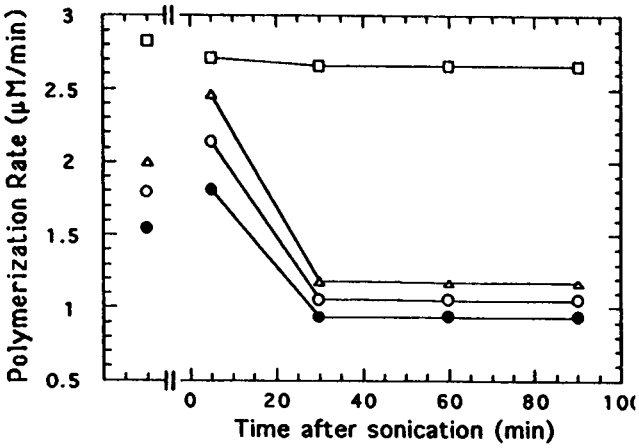

FIGURE 5 Time course of oxidized actin filament annealing after sonication. 0.5-ml aliquots of 12 μM G-actin solutions, previously treated with 0 mM (●, control), 5 mM (○), 10 mM (△), and 20 mM (□) H_2O_2 as described for Fig. 2, were incubated for 24 h in the presence of polymerizing salts (see Materials and Methods) and then sonicated (50 W for 5 s). At 5, 30, 60, and 90 min after disruption, 1.5 ml of 12 μM G-actin (10% pyrene-actin) was added to the sonicated F-actin samples. The rates of nucleated actin polymerization (μM min^{-1}) were calculated as indicated for Fig. 4 and were plotted versus time after sonication. The rates of nucleated polymerizations, before the mechanical fragmentation of F-actin "seeds," have been considered to reflect the steady-state concentration of growing ends in control and oxidized actin samples.

Critical concentration and depolymerization of oxidized actin filaments

Critical concentration for H_2O_2-treated actin polymerization was determined by both "polymerization plateau" and "initial rate" methods (Selden et al., 1986).

Fig. 6 *A* shows the critical concentration (C_c) of oxidized actin samples, as determined by the polymerization plateau method. Briefly, oxidized G-actin samples (total monomer concentration, 2–12 μM, 10% pyrene-actin) were induced to polymerize by the addition of polymerizing salts and incubated up to steady state. The fluorescence intensity of each sample was then measured and plotted versus total actin concentration. The critical concentration value corresponds to the abscissa intercept of the straight line fitting the experimental points. The obtained C_c values were 0.1 μM for control actin and 0.11, 0.28, 0.5 μM for 5, 10, and 20 mM H_2O_2-treated actin samples, respectively.

Critical concentration has also been determined by the initial rate method (Fig. 6 *B*). Small amounts of oxidized filaments (12 μM as a monomer, 10% pyrene-actin) were used to nucleate the assembly of different concentrations of actin monomers (10% pyrene-actin). Net polymerization rates (μM · min^{-1}) for control and oxidized filaments, cal-

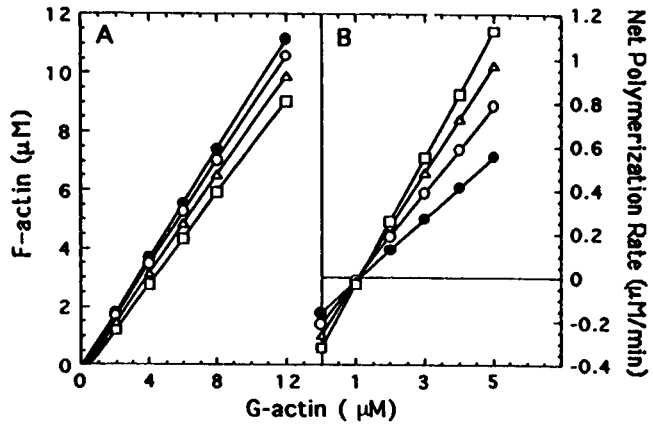

FIGURE 6 Determination of the critical concentration. (*A*) "Polymerization plateau" method. Increasing concentrations (2 to 12 μM) of G-actin (10% pyrene-actin), previously incubated with 0 mM (●, control), 5 mM (○), 10 mM (△), and 20 mM (□) H_2O_2 as described for Fig. 2, were induced to polymerize by the addition of 100 mM KCl + 2 mM $MgCl_2$ (final concentrations). The end points of fluorescence intensity were read after 24 h and plotted versus total actin concentration; the critical concentration is given by the intercept with the abscissa. The critical concentration was 0.1 μM for control actin, and 0.11, 0.28, and 0.5 μM for actin treated with 5, 10 and 20 mM H_2O_2, respectively. (*B*) "Initial rate" method. 0.5-ml aliquots of 12 μM G-actin (10% pyrene-actin), previously incubated with 0 mM (●, control), 5 mM (○), 10 mM (△), and 20 mM (□) H_2O_2 as described for Fig. 2, were polymerized for 24 h in test cuvettes. F-actin samples were then diluted fourfold with increasing concentrations of G-actin (10% pyrene-actin). The final concentrations of polymerizing salts in the assay were 25 mM KCl and 0.5 mM $MgCl_2$. The net polymerization rates (μM min^{-1}) were calculated from the fluorescence intensity changes occurring within the first 2 min and were plotted versus the concentration of added G-actin. The critical concentration is indicated by the intercept with the abscissa and was about 1 μM for both control and H_2O_2-treated samples.

culated from the fluorescence intensity changes occurring within the first 2 min of assembly, have been plotted as a function of the concentration of added G-actin. Critical concentration values (C_c) are given by the intercept of the straight lines, fitting the experimental points, with the x axis. The apparent critical concentration corresponds to the concentration of added G-actin at which the fluorescence intensity does not change, that is, the monomer concentration at which pre-formed filaments neither grow nor shrink. The abscissa intercepts indicate similar C_c values (about 1 μM) for control as well as H_2O_2-treated samples. From Fig. 6, *A* and *B*, we deduced that the critical concentration is not significantly influenced by oxidative injury on actin. Interestingly, differences in critical concentration values have been recorded only by the polymerization plateau method, where polymerization conditions were similar to those used in the experiments reported in Fig. 2 *B* showing the reduction of the polymerization rate in H_2O_2-treated samples.

We finally examined the effect of monomer oxidation on depolymerization of actin filaments. In solution, depolymerization of actin filaments can be induced by diluting the sample to or below the critical concentration. Depolymerization experiments reported in Fig. 7 were carried out by diluting oxidized F-actin samples (20% pyrene-actin) with depolymerizing buffer (G-buffer); depolymerization has been followed by measuring the decrease in fluorescence intensity. From Fig. 7, the maximum depolymerization rate was 0.033 $\mu M \cdot min^{-1}$ for control actin, and 0.046, 0.19, and 0.4 $\mu M \cdot min^{-1}$ for actin treated with 5, 10, and 20 mM H_2O_2, respectively.

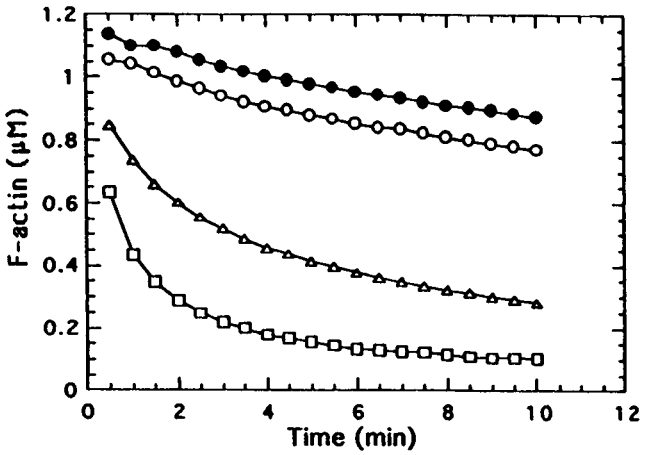

FIGURE 7 Depolymerization rate of oxidized actin filaments. 0.2-ml aliquots of 12 μM G-actin (20% pyrene-actin), previously incubated with 0 mM (●, control), 5 mM (○), 10 mM (△), and 20 mM (□) H_2O_2 as described for Fig. 2, were polymerized in test cuvettes. After 24 h incubation, depolymerization was initiated by diluting the oxidized F-actin samples tenfold with G-buffer (see Materials and Methods). The final concentrations of polymerizing salts in the assay were 10 mM KCl and 0.2 mM $MgCl_2$. The maximum depolymerization rate was 0.033 $\mu M\ min^{-1}$ for control actin, and 0.046, 0.19, and 0.4 $\mu M\ min^{-1}$ for actin treated with 5, 10, and 20 mM H_2O_2, respectively.

Filament free end evaluation at steady state

Small aliquots of H_2O_2-treated G-actin (12 μM) have been induced to polymerize, in test cuvettes, for 24 h, at 25°C. The resulting F-actin samples have then been used to nucleate the polymerization of native G-actin solutions (12 μM; 10% pyrene-actin). The obtained polymerization rates reflect the concentration of free growing ends. Fig. 5 shows that end concentration, at steady state (experimental points before sonication), increases with the oxidant concentration.

Because of both spontaneous fragmentation and annealing, the number of actin filaments (as well as that of growing ends) at steady state does not correspond to the number of polymerization nuclei formed during nucleation. Because H_2O_2 lowers actin nuclei formation and is ineffective on annealing, we suggest that actin filaments from oxidized monomers fragment more easily than control polymers. The presence of more fragmented F-actin, at steady state, was also supported by the higher depolymerization rates shown by H_2O_2-treated actin samples after dilution (Fig. 7) and by electron microscopic analysis (Fig. 9).

Cross-linking of oxidized actin filaments

To reveal the suitability of polymeric actin, formed from oxidized monomers, to interact with accessory proteins, we tested the ability of oxidized actin filaments to form either bundles or networks in the presence of α-actinin and filamin, respectively. Actin bundle formation (Fig. 8 *A*) was followed by light scattering at 400 nm (Wilkins and Lin, 1986). Control and oxidized G-actin samples (9.5 μM) were incubated up to steady state in the presence of increasing α-actinin concentrations and polymerizing salts. The light-scattering intensity of both control and H_2O_2-treated actin

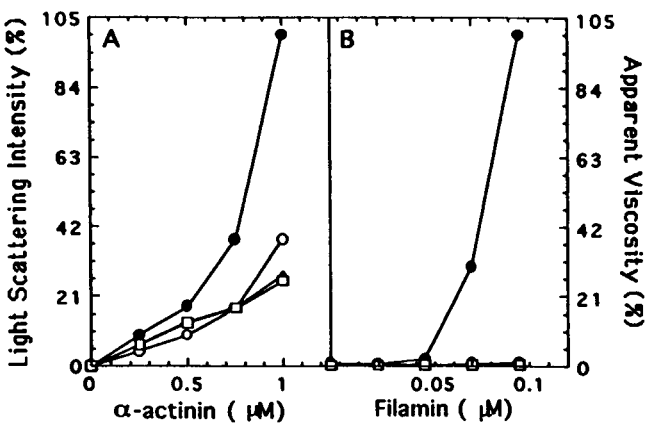

FIGURE 8 Interaction of oxidized actin filaments with α-actinin and filamin. (*A*) 9.5 μM G-actin, previously incubated with 0 mM (●, control), 5 mM (○), 10 mM (△), and 20 mM (□) H_2O_2 as described for Fig. 2, was polymerized (see Materials and Methods) in test cuvettes, in the presence of increasing α-actinin concentrations. (*B*) 7.1 μM G-actin, previously incubated with 0, 5, 10, and 20 mM H_2O_2 as described for Fig. 2, was polymerized in micropipettes (see Material and Methods) in the presence of increasing filamin concentrations. Symbols as for *A*.

samples was plotted as a function of α-actinin concentration (Fig. 8 *A*). Clearly, α-actinin poorly bundles actin filaments formed by H_2O_2-treated actin monomers.

Actin network formation was monitored by low shear viscometry (Pollard and Cooper, 1982). Small aliquots of G-actin (7.1 μM) were polymerized up to steady state in the falling ball micropipettes, in the presence of increasing filamin concentrations. The plot of apparent viscosity values versus filamin concentrations (Fig. 8 *B*) shows that filamin fails to cross-link oxidized actin polymers, at all the tested conditions.

It is important to underline that cosedimentation assays (not shown) demonstrated that only filamin markedly lowers its affinity for oxidized actin filaments. The filamin/oxidized F-actin ratio dropped from 70% to 20% of that of controls, with the increase of the oxidative stress. The α-actinin/oxidized F-actin ratio, in contrast, was unaffected.

DISCUSSION

H_2O_2-treated G-actin shows an altered time course of assembly. Both light-scattering (Fig. 2 *A*) and fluorimetric (Fig. 2 *B*) experiments showed evidence of the increase in the lag phase and the decrease of both the maximum polymerization rate and the polymerization extent. All of the observed effects are dose-related, because they increase with the enhancement of the oxidative stress. Furthermore, the H_2O_2 injury on actin is not merely associated with the protein denaturation, because of the lack of the characteristic spectral redshift (not shown) (Kerwar and Lehrer, 1972; Gershman et al., 1988; Kinosian et al., 1993). G-actin likely gets several oxidable sites with different sensitivities to hydrogen peroxide. After the treatment of G-actin samples with different concentrations of H_2O_2, heterogeneous populations of differently injured actin molecules probably form. In particular, with the increase in H_2O_2 concentration, the number of actin molecules showing assembly troubles increases. This agrees with both the reduced nucleation shown in Fig. 3 and the lowering in elongation rates documented in Fig. 4.

Fig. 5 and Fig. 6, *A* and *B*, suggest that neither the annealing of short actin polymers into longer ones nor the critical concentration of steady-state actin samples seem to be markedly affected by the treatment of actin with hydrogen peroxide. We detected small changes in the critical concentration only by using the polymerization plateau method (Fig. 6 *A*), where polymerization conditions were similar to those used in time-course experiments (Fig. 2 *B*). In contrast, the initial rate method did not reveal any change in C_c values (Fig. 6 *B*). These facts suggest that only a negligible number of H_2O_2-treated monomers fail to polymerize; most of the oxidized actin molecules merely lower their tendency to assemble. The influence of hydrogen peroxide on actin assembly does not represent an "all or nothing" effect.

The key point on which to build an explanation of the molecular mechanism(s) driving the activity of hydrogen peroxide on actin cytoskeleton lies in the characteristics of actin filaments assembled from H_2O_2-treated actin monomers. Fig. 5 clearly shows that steady-state actin samples, whose monomers have been treated with 20 mM H_2O_2, are insensitive to sonication. Their end concentration (i.e., number of filaments), in fact, did not change after mechanical stress, remaining markedly high at all of the tested time points after sonication. This could mean that the 20 mM H_2O_2-treated actin samples are characterized by the presence of short actin polymers, which fail to further fragment under sonication. Data summarized in Figs. 5 and 7 lead to a similar conclusion. The polymerization of fluorescently labeled actin samples, when nucleated with F-actin from oxidized monomers, reveals the higher fragmentation of the added actin polymers (Fig. 5, experimental points before sonication). The enhancement of filament ends is only partially related to the increase in the oxidant concentration but, undoubtedly, the stronger the oxidative treatment, the more fragmented is the steady-state F-actin. Depolymerization experiments gave similar results (Fig. 7). The depolymerization rate is a function of the number of sites (i.e., filament ends) where actin subunits are released. The number of actin filaments at steady state is enhanced with the increase in H_2O_2 concentration used for the treatment of actin monomers. Moreover, because the total mass of polymer steady state does not increase, actin filaments should be shorter in treated samples than in controls.

The fragility of actin polymers assembled from H_2O_2-treated monomers could be due to the weakness of the bonds between actin subunits. Three-dimensional reconstructions of the actin filaments (Milligan et al., 1990) together with NMR studies (Barden et al., 1989) predicted that Cys-374, at the C-terminus of the actin molecule, is close to the intermolecular interface on actin. Electron micrographs of filaments composed of truncated actins, devoid of the last two (O'Donoghue et al., 1992) or three (Mossakowska et al., 1993) C-terminal residues, indicate an increased flexibility and fragility of the polymer. This suggests that C-terminal residues of actin sequence are crucial for filament strength as well as for intermonomer communications. It is well known that Cys-374 shows one of the more reactive sulfhydryl groups of the actin molecule. Many of different actin labeling procedures (Kouyama and Mihashi, 1981; Tait and Frieden, 1982; Cooper et al., 1983) are carried out by chemical modifications of Cys-374. However, the labeling of actin molecules easily occurs with F-actin, whereas it is more difficult when G-actin is used.

In our opinion, one of the effects of hydrogen peroxide on actin could involve the modification of actin monomers at their C-terminus, likely by the oxidation of the Cys-374 sulfhydryl group; in fact, our measurements showed an average loss of two sulfhydryl groups in H_2O_2-treated actin. Oxidation could not involve all actin molecules in the sample, because of the relative inaccessibility of Cys-374 on monomeric actin. This could also explain the interrelationship between the strength of oxidative injury and the extent of hydrogen peroxide effects on actin. During the assembly

of H_2O_2-treated actin monomers, the lowered actin nuclei formation, the partial inhibition of the elongation step, as well as the marked fragmentation of polymers at steady state could be ascribed to the difficulty of formation of intermonomer bonds by C-terminus-altered actin molecules.

Crosbie et al. (1994) demonstrated that actin's C-terminus is structurally coupled to other distant parts of the protein. Furthermore, they suggested that the C-terminus is an important region for determining actin structure and modulating its function by several actin-binding proteins. These suggestions are in excellent agreement with the data reported in Fig. 8, *A* and *B*. Actin filaments, from the assembly of H_2O_2-treated monomers, do not form networks in the presence of filamin (Fig. 8 *B*) and poorly bundle in the presence of α-actinin (Fig. 8 *A*), confirming that the presence of altered actin subunits could rearrange the whole structure of the filament. For example, McGough et al. (1994) suggested that α-actinin binds together the subdomain 1 of two adjacent actin subunits along the so-called long-pitch helix (Egelman, 1985) of the actin filament; most actin-cross-linking proteins, belonging to the spectrin superfamily (such as α-actinin, filamin, etc.), bind the subdomain 1 of actin monomers, where the C-terminus of actin molecule is located (Kabsch et al., 1990). Our results could be partially explained by the "structural connectivity in actin," whose relevance for actin dynamics has been elegantly demonstrated by Crosbie et al. (1994). Nevertheless, we have to consider that mechanical characteristics of actin networks depend on the binding ability of the cross-linker versus actin polymers as well as on the length of involved actin filaments. As shown by electron microscopy (Fig. 9), the reduction of filament size in H_2O_2-treated samples is appreciable but not dramatic. In parallel, cosedimentation assays (not shown) demonstrated that only filamin shows a marked reduction of binding versus oxidized F-actin. Considering these results, filamin completely fails to form actin networks because of the concomitant influence of both the reduced length of oxidized actin filaments and the drop of its affinity to oxidized actin polymers. In contrast, α-actinin/oxidized F-actin interaction is mainly affected by the reduced size of H_2O_2-treated actin filaments.

In conclusion, H_2O_2-treated G-actin, because of its difficulty in establishing intermonomer bonds, shows a low nucleation activity, a slackening of the elongation, as well as a more fragmented polymer mass at steady state. All of these characteristics are ascribable to the unstable structure of actin filaments, assembled from oxidized monomers.

We have to underline some discrepancies existing between our results and those obtained by other researchers on cultured cells. In particular, we refer to the lack of correlation between the increase in cell F-actin content and the actin nucleation activity, observed by Omann et al. (1994) in a transformed murine macrophage cell line (where the H_2O_2-induced F-actin increases correlate with a decrease in actin nucleation activity). This fact is really anomalous, as pointed out by the authors themselves. Considering that, in the presence of hydrogen peroxide, actin polymers tend to fragment (this phenomenon has been observed, in vivo, by Hinshaw et al., 1986, 1988, 1991, and further confirmed in this paper), in H_2O_2-treated cells the actin nucleation activity should increase. Omann and colleagues failed to show evidence for a direct correlation between the increase in cytoplasmic F-actin and the lowering of actin nucleation activity, because of the deep differences in sample handling characterizing the different applied techniques. Before cytochemical F-actin staining, cell fixation procedures tend to "freeze" the cytoplasmic F-actin pattern, whereas, in contrast, short unstable actin filaments could be easily reduced in number or completely disassemble during biochemical cell fractioning. Furthermore, Omann et al. (1994) stated that oxidized actin is still capable of polymerizing because pyrene-actin, with the pyrene moiety attached to Cys-374, does it. This deduction could be substantially correct, but it does not take into account possible assembly differences related to the nature of the chemical modification. Because of the "structural connectivity" in actin, modifications induced at any site of the actin molecule could be structurally transmitted to distant regions of the monomer, but the type of the transmitted "signal" strictly depends on the nature of the modifying agent (Crosbie et al., 1994). For this

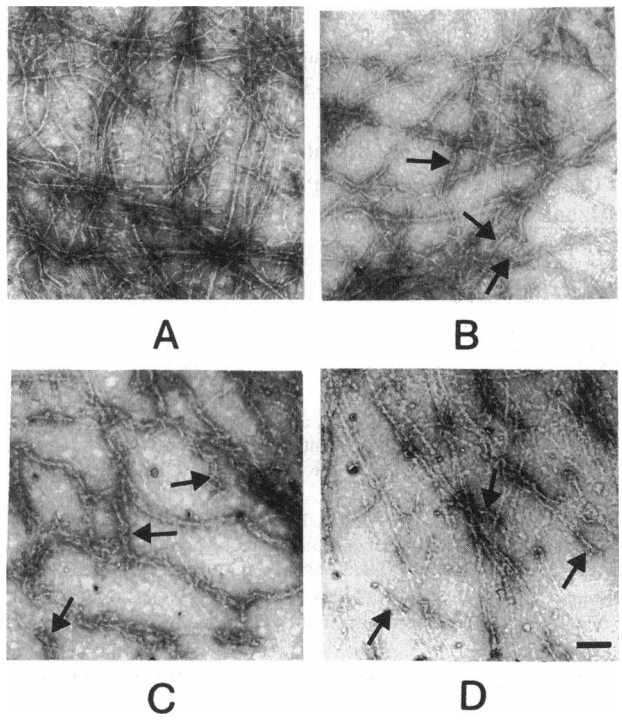

FIGURE 9 Electron micrographs of F-actin samples from oxidized actin monomers. (*A*) Control actin filaments. (*B*) Actin polymers from 5 mM H_2O_2-treated actin monomers. (*C*) Actin polymers from 10 mM H_2O_2-treated G-actin. (*D*) Actin polymers from 20 mM H_2O_2-treated actin monomers. Arrows indicate short actin polymers in oxidized actin samples. Bar = 100 nm

reason, pyrene-actin, *N*-ethylmaleimide–actin, and *N*-(iodoacetyl)-*N'*-(5-sulfo-1-naphthyl)ethylenediamine-actin (all actins modified at Cys-374) show different assemby kinetics (Tait and Frieden, 1982; Cooper et al., 1983; Crosbie et al., 1994) and, above all, marked differences in the binding of accessory proteins (Crosbie et al., 1994; Milzani et al., 1995).

REFERENCES

Barden, J. A., L. Phillips, B. A. Cornell, and C. G. dosRemedios. 1989. ^{19}F NMR studies of the interaction of selectively labeled actin and myosin. *Biochemistry.* 28:5895–5901.

Bellomo, G., S. A. Jewell, H. Thor, and S. Orrenius. 1982. Regulation of intracellular calcium compartmentation: studies with isolated hepatocytes and t-butyl hydroperoxide. *Proc. Natl. Acad. Sci. USA.* 79: 6842–6846.

Carlier, M.-F., D. Pantaloni, and E. D. Korn. 1984. Evidence of an ATP cap at the end of actin filaments and its regulation of the F-actin steady state. *J. Biol. Chem.* 259:9983–9986.

Colombo, R., A. Milzani, P. Contini, and I. DalleDonne. 1991a. Lithium effects on actin polymerization in the presence of magnesium. *Biochem. J.* 274:421–425.

Colombo, R., A. Milzani, and I. DalleDonne. 1991b. Lithium increases actin polymerization rates by enhancing the nucleation step. *J. Mol. Biol.* 217:401–404.

Cooper, J. A., S. B. Walker, and T. D. Pollard. 1983. Pyrene actin: documentation of the validity of a sensitive assay for actin polymerization. *J. Muscle Res. Cell Motil.* 4:253–262.

Crosbie, R. H., C. Miller, P. Cheung, T. Goodnight, A. Muhlrad, and E. Reisler. 1994. Structural connectivity in actin: effect of C-terminal modifications on the properties of actin. *Biophys. J.* 67:1957–1964.

Egelman, E. H. 1985. The strcture of F-actin. *J. Muscle Res. Cell Motil.* 6:129–151.

Ellman, G. L. 1959. Tissue sulfhydryl groups. *Arch. Biochem. Biophys.* 82:70–77.

Elzinga, M., and J. H. Collins. 1975. The primary structure of actin from rabbit skeletal muscle. *J. Biol. Chem.* 250:5897–5905.

Feramisco, J. R., and Burridge, K. 1980. A rapid purification of α-actinin, filamin and a 130,000 daltons protein from smooth muscle. *J. Biol. Chem.* 255:1194–1199.

Frieden, C., and D. W. Goddette. 1983. Polymerization of actin and actin-like system: evaluation of the time course of polymerization in relation to the mechanism. *Biochemistry.* 22:5836–5843.

Gershman, L. C., J. E. Estes, and L. A. Selden. 1988. Polymerization characteristics of divalent cation-free actin. *Ann. N.Y. Acad. Sci.* 259: 264–266.

Gordon, D. J., Y. Z. Yang, and E. D. Korn. 1976. Polymerization of *Acanthamoeba* actin. *J. Biol. Chem.* 251:7474–7479.

Hinshaw, D. B., B. C. Armstrong, J. M. Burger, T. F. Beals, and P. A. Hyslop. 1988. ATP and microfilaments in cellular oxidant injury. *Am. J. Pathol.* 132:479–488.

Hinshaw, D. B., J. M. Burger, T. F. Beals, B. C. Armstrong, and P. A. Hyslop. 1991. Actin polymerization in cellular oxidant injury. *Arch. Biochem. Biophys.* 288:311–316.

Hinshaw, D. B., L. A. Sklar, B. Bohl, I. U. Schraufstatter, P. A. Hyslop, M. W. Rossi, R. G. Spragg, and C. G. Cochrane. 1986. Cytoskeletal and morphologic impact of cellular oxidant injury. *Am. J. Pathol.* 123: 454–464.

Holeysovsky, V., and M. Lazdunski. 1968. The structural properties of trypsinogen and trypsin. Alkylation and oxidation of methionines. *Biochem. Biophys. Acta.* 154:457–467.

Jewell, S. A., G. Bellomo, H. Thor, S. Orrenius, and M. T. Smith. 1982. Bleb formation in hepatocytes during drug metabolism is caused by disturbances in thiol and calcium ion homeostasis. *Science.* 217: 1257–1259.

Kabsch, W., H. G. Mannherz, D. Suck, E. F. Pai, and K. C. Holmes. 1990. Atomic structure of the actin: DNase I complex. *Nature.* 347:37–44.

Kawamura, M., and K. Maruyama. 1970. Electron microscopic particle length of F-actin polymerized in vitro. *J. Biochem.* 67:437–457.

Kerwar, G., and S. S. Lehrer. 1972. Intrinsic fluorescence of actin. *Biochemistry.* 11:1211–1217.

Kinosian, H. J., L. A. Selden, J. E. Estes, and L. C. Gershman. 1993. Nucleotide binding to actin: cation dependence of nucleotide dissociation and exchange rates. *J. Biol. Chem.* 268:8683–8691.

Knight, P., and G. Offer. 1978. *p-N,N'*-Phenylenebismaleimide, a specific cross-linking agent for F-actin. *Biochem. J.* 175:1023–1032.

Korn, E. D. 1985. The regulation of actin and myosin by ATP. *Curr. Top. Cell. Regul.* 26:221–232.

Kouyama, T., and K. Mihashi. 1981. Fluorimetry study of N-(1-pyrenyl)iodoacetamide-labelled F-actin. *Eur. J. Biochem.* 114:33–38.

Laemmli, U. K. 1970. Cleavage of structural proteins during assembly of the head of bacteriophage T4. *Nature.* 227:680–685.

Martin, W. J., II. 1984. Neutrophils kill pulmonary endothelial cells by a hydrogen peroxide dependent pathway. *Am. Rev. Respir. Dis.* 130: 209–213.

McGough, A., M. Way, and D. DeRosier. 1994. Determination of the α-actinin-binding site on actin filaments by cryoelectron microscopy and image analysis. *J. Cell Biol.* 126:433–443.

Mesland, D. A. M., G. Los, and H. Spiele. 1981. Cytochalasin B disrupts the association of filamentous web and plasma membrane in hepatocytes. *Exp. Cell. Res.* 135:431–435.

Milligan, R. A., M. Whittaker, and D. Safer. 1990. Molecular structure of F-actin and location of surface binding sites. *Nature.* 348:217–221.

Millonig, R., H. Salvo, and U. Aebi. 1988. Probing actin polymerization by intermolecular cross-linking. *J. Cell Biol.* 106:785–796.

Milzani, A., I. DalleDonne, and R. Colombo. 1995. N-Ethylmaleimide-modified actin filaments do not bundle in the presence of α-actinin. *Biochem. Cell Biol.* 73:116–122.

Mirabelli, F., A. Salis, V. Marinoni, G. Finardi, G. Bellomo, H. Thor, and S. Orrenius. 1988. Menadione-induced bleb formation in hepatocytes is associated with the oxidation of thiol groups in actin. *Arch. Biochem. Biophys.* 264:261–269.

Mossakowska, M., J. Moraczewska, S. Khaitlina, and H. Strzelecka-Golaszewska. 1993. Proteolytic removal of three C-terminal residues of actin alters the monomer-monomer interactions. *Biochem. J.* 289: 897–902.

Murphy, D. B., R. O. Gray, W. A. Grasser, and T. D. Pollard. 1988. Direct demonstration of actin filament annealing in vitro. *J. Cell Biol.* 106: 1947–1954.

Nakaoka, Y., and M. Kasai. 1969. Behaviour of sonicated actin polymers: adenosine triphosphate splitting and polymerization. *J. Mol. Biol.* 44: 319–332.

Nathan, C. F., S. C. Silverstein, L. H. Breckner, and Z. A. Cohn. 1979. Extracellular cytolysis by activated macrophages and granulocytes. II. Hydrogen peroxide as a mediator of cytotoxicity. *J. Exp. Med.* 149: 100–113.

Neumann, N. P. 1972. Oxidation with hydrogen peroxide. *Methods Enzymol.* 25:393–400.

O'Donoghue, S. I., M. Miki, and C. G. dosRemedios. 1992. Removing the two C-terminal residues of actin affects the filament structure. *Arch. Biochem. Biophys.* 293:110–116.

Omann, G. M., J. M. Harter, J. M. Burger, and D. B. Hinshaw. 1994. H_2O_2-induced increases in cellular F-actin occur without increases in actin nucleation activity. *Arch. Biochem. Biophys.* 308:407–412.

Oosawa, F., and M. Kasai. 1971. Actin. *In* Subunits in Biological Systems, part A. S. Timasheff and G. D. Fasman, editors. Marcel Dekker, New York. 261–322.

Pollard, T. D., and J. A. Cooper. 1982. Methods to characterize actin filament networks. *Methods Enzymol.* 85:211–233.

Prentki, M., C. Chaponnier, B. Janrenaud, and G. Gabbiani. 1979. Actin microfilaments, cell shape, and secretory processes in isolated rat hepatocytes. Effect of phalloidin and cytochalasin D. *J. Cell Biol.* 81: 592–607.

Sacks, T., C. F. Moldow, P. R. Craddock, T. K. Bowers, and H. S. Jacobs. 1978. Oxygen radicals mediate endothelial cell damage by complement-stimulated granulocytes: an in vitro model of immune vascular damage. *J. Clin. Invest.* 61:1161–1167.

Schraufstatter, I. U., D. B. Hinshaw, P. A. Hyslop, R. G. Spragg, and C. G. Cochrane. 1985. Glutathione cycle activity and pyridine nucleotide levels in oxidant induced injury of cells. *J. Clin. Invest.* 76:1131–1129.

Schraufstatter, I. U., D. B. Hinshaw, P. A. Hyslop, R. G. Spragg, and C. G. Cochrane. 1986. Oxidant injury of cells: DNA strand breaks activate polyadenosine diphosphate-ribose polymerase and lead to depletion of nicotinamide adenine dinucleotide. *J. Clin. Invest.* 77:1312–1320.

Selden, L. A., L. C. Gershman, and J. E. Estes. 1986. A kinetic comparison between Mg-actin and Ca-actin. *J. Muscle Res. Cell Motil.* 7:215–224.

Shizuta, Y., H. Shizuta, M. Gallo, P. Davies, I. Pastan, and M. S. Lewis. 1976. Purification and properties of filamin, an actin binding protein from chicken gizzard. *J. Biol. Chem.* 251:6562–6567.

Simon, R. H., C. H. Scoggin, and D. Patternson. 1981. Hydrogen peroxide causes the fatal injury to human fibroblasts exposed to oxygen radicals. *J. Biol. Chem.* 256:7181–7186.

Spragg, R. G., D. B. Hinshaw, P. A. Hyslop, I. U. Schraufstatter, and C. G. Cochrane. 1985. Alterations in adenosine triphosphate and energy energy change in cultured endothelial and P388D_1 cells following oxidant injury. *J. Clin. Invest.* 76:1471–1476.

Spudich, J. A., and S. Watt 1971. The regulation of rabbit skeletal muscle contraction. Biochemical studies on the interaction of the tropomyosin-troponin complex with actin and the proteolytic fragments of myosin. *J. Biol. Chem.* 246:4866–4871.

Suzuki, A., D. E. Goll, I. Singh, R. E. Allen, R. Robson, and M. H. Stromer. 1976. Some properties of purified skeletal muscle α-actinin. *J. Biol. Chem.* 251:6860–6870.

Tait, J. F., and C. Frieden. 1982. Chemical modification of actin. Acceleration of polymerization and reduction of network formation by reaction with *N*-ethylmaleimide, (iodoacetamido)tetramethylrhodamine, or 7-chloro-4-nitro-2,1,3-benzoxadiazole. *Biochemistry.* 21:6046–6053.

Tellam, R., and C. Frieden. 1982. Cytochalasin D and platelet gelsolin accelerate actin polymer formation: a model for regulation of the extent of actin polymer formation in vivo. *Biochemistry.* 21:3207–3214.

Trump, B. F., and W. J. Mergner. 1974. Cell Injury, Vol. 1, The Inflammatory Process, 2nd edition. B. W. Zweitach, L. Grant, and R. T. McCluskey, editors. Academic Press, New York. 115–257.

Wang, K., J. F. Ash, and S. J. Singer. 1975. Filamin, a new high molecular weight protein found in smooth muscle and non-muscle cells. *Proc. Natl. Acad. Sci. USA.* 72:4483–4486.

Wegner, A., and P. Savko. 1982. Fragmentation of actin filaments. *Biochemistry.* 21:1909–1913.

Weiss, S. J., J. Young, A. F. LoBuglio, and K. A. Slivka. 1981. Role of hydrogen peroxide in neutrophil-mediated destruction of cultured endothelial cells. *J. Clin. Invest.* 68:714–724.

Wilkins, J. A., and S. Lin. 1986. A re-examination of the interaction of vinculin with actin. *J. Cell Biol.* 102:1085–1092.